Transiently elevated expression of different forms of brain-derived neurotrophic factor in the neonatal medial prefrontal cortex affected anxiety and depressive-like behaviors in adolescence

Dmitriy Lanshakov[1,2], Elizaveta Shaburova[1], Ekaterina Sukhareva[1], Veta Bulygina[3], Uliana Drozd[1], Irina Larionova[4], Tatiana Gerashchenko[4], Tatiana Shnaider[5], Evgeny V. Denisov[4] and Tatyana Kalinina[2,3]

[1] Postgenomics Neurobiology Laboratory, Institute of Cytology and Genetics, Novosibirsk, Russia
[2] Novosibirsk State University, Novosibirsk, Russia
[3] Functional Neurogenomics Laboratory, Institute of Cytology and Genetics, Novosibirsk, Russia
[4] Laboratory of Cancer Progression Biology, Tomsk National Research Medical Center, Tomsk, Russia
[5] Sector of Genomic Mechanisms of Ontogenesis, Institute of Cytology and Genetics, Novosibirsk, Russia

ABSTRACT

Brain-derived neurotrophic factor (BDNF) is a secreted molecule that plays an important role in the survival and growth of nerve cells. BDNF undergoes complex post-translational processing with cellular proteases. Pro- and mature BDNF forms bind to different receptor types in the brain. BDNF is prominent in the neonatal cerebral cortex. The neonatal period is critical for the proper development of the brain and nervous system. Disruptions in these critical periods can have long-lasting effects on behavior and mental health. Individuals who experience adverse effects in the neonatal period have demonstrated a predisposition to depression and other neurobehavioral disorders. In this work we studied the influence of transient expression (P3–P8) elevation of pro-, mature and mutant forms of BDNF that could not be processed with cellular convertases in the neonatal medial prefrontal cortex (mPFC) on anxiety and depressive-like behavior in adolescents. Elevated expression of mature BDNF (LV-BDNF) increased anxiety and depressive-like behavior at P30. Only immobility in the tail suspension test was increased after expression of mutant BDNF (LV-pBDNF mut). Using our RNA-seq data and available online sn-RNAseq results, we investigated transcriptomic changes in the neonatal mPFC at P8 that underlie subsequent behavioral changes. Mature BDNF expression caused an increased transcriptional response in perivascular stromal cells (PSC) with such genes: *Ptgds, Slc6a13, Slc22a6, Bnc2, Slc13a4, Aldh1a2*. Based on GWAS data, Ptgds is a candidate gene associated with ADHD and bipolar disorder *Pujol-Gualdo et al. (2021)*; *Marín-Méndez et al. (2012)*; *Munkholm et al. (2015)*. LV-pBDNF mut caused a complete opposite set of transcriptional changes in the PSC compared to LV-BDNF. The observed similar behavioral phenotype after expression of mature and mutant forms of BDNF together with the detected genes related to bipolar disorder underpinned that *Bdnf* could play a substantial role in the pathogenesis of this neurobehavioral disorder.

INTRODUCTION

Brain maturation is a complex and intricate process that takes considerable time to develop. Several shifts of main lead programs occurred during this multiplexing process (*Zhong et al., 2018*; *Amiri et al., 2018*; *Polioudakis et al., 2019*). First neurogenesis gives way to astro-, then oligodendrogenesis and synaptogenesis (*Zhong et al., 2018*; *Amiri et al., 2018*; *Polioudakis et al., 2019*). Changes in key processes are accompanied by changes in cell dynamics and transcriptomics. The early neonatal period is crucial for further brain development and mental abilities (*Lanshakov et al., 2016*). Harmful and stressful effects during these periods have long-lasting consequences on mental health and abilities. It has been brilliantly demonstrated in monocular deprivation experiments in the early postnatal period and the lifelong consequences of such effects (*Fong et al., 2016*; *Pizzorusso et al., 2006*). During the neonatal period, neural circuits are tuned and developed (*Luhmann et al., 2016*).

Maternal stress during pregnancy, adverse early life experiences may predispose individuals to develop psychopathology in adulthood (*Satinsky et al., 2021*; *Xia et al., 2023*). Another factor that affects the developing nervous system and is commonly encountered in perinatal medicine is antenatal glucocorticoid therapy, which is prescribed to women at risk of preterm delivery. We have previously shown that administration of the synthetic glucocorticoid dexamethasone causes neuronal apoptosis in the subiculum of neonatal rat pups (*Lanshakov et al., 2016*). Maternal behavior and early environmental conditions could affect offspring brain maturation through DNA methylation and epigenetic mehanisms (*Weaver et al., 2004*) involving *Bdnf* exon IV differential transcription in the prefrontal cortex (PFC) (*Costa et al., 2023*).

If we were to talk about genes and factors that orchestrate central nervous system (CNS) development and cross-talk with environmental factors, we should first talk about neurotrophic factors or *Bdnf*. *Bdnf* is a secreted neurotrophic factor with complex expression regulation and protein processing (*Mowla et al., 2001*; *Menshanov, Lanshakov & Dygalo, 2015*). First, its mRNA is translated into preproform, which is processed by cellular proteases into proform (*Menshanov, Lanshakov & Dygalo, 2015*). Furin and several other cell convertases then cleave the proform to mature BDNF. proBDNF and matBDNF mostly bind to different receptor types in the brain (*Menshanov, Lanshakov & Dygalo, 2015*). Proform binds to the p75NTR and sortilin/SorCS1-3 coreceptors (*Glerup, Nykjaer & Vaegter, 2014*; *Glerup et al., 2014*; *Glerup et al., 2016*; *Kraemer et al., 2014*; *Leloup, Chataigner & Janssen, 2018*), and mature form binds to TrkB–kinase receptor (*Minichiello, 2009*). p75NTR and TrkB have different receptor pathways and may have different effects on behavior in addition to their roles in neuronal plasticity and synapse formation (*Glerup et al., 2016*; *Glerup, Nykjaer & Vaegter, 2014*; *Glerup et al., 2014*; *Kraemer et al., 2014*; *Leloup, Chataigner & Janssen, 2018*; *Minichiello, 2009*; *Marchetti et al., 2019*; *Rezgaoui et al., 2001*).

We are far from a complete understanding of the precise molecular mechanisms of action of proBDNF and matureBDNF in the neonatal brain. Alteration of pro- and mature BDNF signaling during the early postnatal period could have a long-lasting outcome on mental health and predisposition to anxiety and depression in adulthood. Medial prefrontal cortex (mPFC) neuronal activity and BDNF signaling play key role in resisting depression (*Hare & Duman, 2020*). Opposite changes in BDNF expression are observed in the brains of patients with major depression. Upregulation of BDNF occurs in the amygdala and nucleus accumbens, while downregulation of BDNF occurs in the hippocampus and medial prefrontal cortex (mPFC) (*Phillips, 2017*). From a receptor perspective, experiments with TrkB and TrkBT1 have also had opposite results on anxiety and depression. Mice overexpressing TrkBT1 (*i.e.* reduced BDNF signaling) showed decreased exploratory activity (*Kemppainen et al., 2012*), whereas mice lacking TrkBT1 (*i.e.* increased BDNF signaling) showed increased anxiety (*Watson et al., 2015*). BDNF abnormalities also contribute to astrocyte and microglial dysfunction in depression pathways (*Phillips, 2017*). During the first postnatal week, *Bdnf* is expressed in the hippocampus and mPFC of rodents (*Mowla et al., 2001*; *Baquet, Gorski & Jones, 2004*).

It is hypothesized that proBDNF plays opposite roles to mature BDNF in neuronal functions. To address this question and the role of pro- and mature BDNF in the neonatal prefrontal cortex, we used several methods: viral transduction, RNA-seq, and behavioral assays. Using an all in one Tet-ON doxycycline (DOX)-inducible system, we temporally increased the expression of different BDNF forms, in particular: mature BDNF, proBDNF, and proBDNF mutant form, where the convertase cleavage site was mutated -126RVRR129 →-126AAAA129. It could not be processed by Furin because of this mutation. After expression activation during the first postnatal week, RNA sequencing was performed to assess transcriptomic changes caused by different BDNF forms. To correlate transcriptomic changes with behavioral changes following increased expression of different forms of BDNF in the neonatal mPFC, anxiety and depressive-like behaviors were examined at P30 in adolescents. The present paper shows the major target genes of BDNF and proBDNF signaling in the neonatal mPFC. Temporal alteration of BDNF signaling in the neonatal mPFC had a significant effect on anxiety and depressive-like behaviors in adolescence.

MATERIALS AND METHODS

Constructs

To create an all-in-one TET-ON lentiviral vector (LV) specifically expressed in neurons, the hPGK promoter was replaced with the hSyn promoter in the plasmid pCW57-MCS1-P2A-MCS2(GFP). This was done using two-step cloning. pCW57-MCS1-P2A-MCS2(GFP) was a gift from Adam Karpf (Addgene plasmid 80924; http://n2t.net/addgene: 80924; RRID:Addgene_80924). First, pCW57-MCS1-P2A-MCS2 (GFP) was cleaved with AsuNHI/FspI, then the 155bp fragment was ligated to the 7237bp fragment obtained after pCW57-MCS1-P2A-MCS2(GFP) was cleaved with AsuNHI/HindII. Second, in the result, promoterless construct human synapsin promoter (hSyn) was cloned with MluI/BamHI sites, resulting in pCW57-MCS1-P2A-MCS2-hSyn(GFP)

construct (*Shaburova & Lanshakov, 2021*). The hSyn sequence was taken from the plasmid pAAV-hSyn-hChR2(H134R)-mCherry. pAAV-hSyn-hChR2(H134R)-mCherry was a gift from Karl Deisseroth (Addgene plasmid 26976; Available at http://n2t.net/addgene:26976; RRID:Addgene_26976). The cDNAs encoding proBDNF were amplified from the cDNA library of rat P4 brain pups using the primers listed in Table S1. The PCR product was T/A cloned into the pAL-TA (Evrogen) vector and verified by Sanger sequencing. Using PCR directed mutagenesis and primers from Table S1, the cleavage site and HAtag mutations were introduced. All intermediates have been T/A cloned. Subsequently, AsuNHI and SalI sites were introduced by PCR and sequences encoding different forms of BDNF were cloned into pCW57-MCS1-P2A-MCS2-hSyn(GFP).

Animals

All animal procedures were approved by the Animal Care and Use Committee of the Institute of Cytology and Genetics (Protocol 151 dated 28.04.2023) and were performed in accordance with the European Communities Council Directive 63/2010/EU. Animals were obtained from the conventional animal facility of the Institute of Cytology and Genetics. Gestational Wistar rats were individually housed at 22–24 °C, 12-hour dark/12-hour light cycle, ad libitum. Birth date was considered P0. The litters were limited to a maximum of 8 male puppies per litter. The remainder were crossbred from other dams if there were less than 8 males in the litter. The same litter contained animals from all of the experimental groups in a randomized fashion. To distinguish the baby rats, they were marked with red paint (fucorcin) on the right front paw, right side, right rear paw, tail base, left rear paw, left side, left front paw, head, according to the numbers from 1 to 8. The tags were updated on a daily basis. On P24, the mothers were removed. After weaning, the animals were housed in groups of 4 per cage. All experimental samples were blindly number-coded for further processing.

Cell transfection and western blotting

CHO-K1 cells (obtained from the cell culture collection of the State Research Center of Virology and Biotechnology Vector, Novosibirsk, Russia) were cultured in DMEM/F12 medium supplemented with 10% FBS, 1X NEAA, 1 mM L-glutamine, 50 U/ml penicillin, and 50 mg/ml streptomycin. The day before transfection, CHO-K1 cells were seeded on a 48-well plate with a density of $3.5 * 10^4$ cells per cm^2. The next day, cells were transfected with 0.5 µg of plasmid DNA per well and Lipofectamine 3000, dissolved in DMEM/F12, according to the manufacturer's instructions. The next morning, a fresh growth medium was added. Half of all samples had DOX in the medium at a concentration of 20 ng/ml. After 1 hour of incubation, the medium was removed and the cells were washed once with warm 1xPBS. After that 200 µl RIPA lysis buffer (50 mM Tris pH 7.4, 0.1% SDS, 0.5% sodium deoxycholate, 1.0% NP-40, 1.0% Triton X-100, 150 mM NaCl) together with 1x Protease Inhibitor Cocktail (P2714, Sigma Aldrich) was added in each well and cells were scraped. For the proper lysis and dis-aggregation samples were passed through 10 strokes of insulin syringe with 29Ga needle. Cell debris was then removed by centrifuging at 12,000 g for 10 minutes at 4 °C. The Lowry assay was used to measure protein concentration.

Lysates containing 20 μg of total protein were denatured at 95 ° for 5 min in 1x Laemli buffer (50 mM Tris-HCl (pH 6.8), 10% glycerol, 100 mM β-mercaptoethanol, 1% SDS, 0.002% bromophenol blue). They were then loaded onto an Any kD Mini-PROTEAN TGX Stain-Free Protein Gel (Bio-Rad, Hercules, CA, USA) and run at 100 V for 1 hour in running buffer (25 mM Tris, 192 mM glycine, 0.1% SDS, pH 8.3). The proteins were then transferred to 0.2 μm nitrocellulose membrane (Bio-Rad, Hercules, CA, USA) using the following parameters: 100 V, 20 min in transfer buffer (47.9 mM Tris, 38.6 mM glycine, 20% methanol, pH8.3). Membranes were blocked for 1 hour at RT in 0.5% fish skin gelatine 0.1% bovine casein in 1xPBS with 0.1% Triton X-100 (1xPBST) and incubated overnight at 4 °C with anti-HA-tag primary antibody (SAB4300603, Sigma-Aldrich, St. Louis, MO, USA) diluted 1:2,000 in Sea Block (37527, Thermo Fisher Scientific, Waltham, MA, USA). The next day, the membranes were washed in 1xPBS 0.1% SDS and incubated with secondary antibody (goat anti-rabbit IgG; Bio-Rad, Hercules, CA, USA) 1:5,000 diluted in blocking buffer for 1 hour at RT. SuperSignal West Femto Maximum Sensitivity Substrate (Thermo Fisher Scientific, Waltham, MA, USA) was used to amplify the chemiluminescence signal. The membranes were imaged using the Chemidoc Touch Imaging System (Bio-Rad, Hercules, CA, USA) and the staining intensity of the bands corresponding to the analyzed proteins was evaluated. The membranes were then stripped for 30 min at 50°C in harsh stripping buffer 2% SDS 62mM Tris HCl pH =6.8 0.8% ß-mercaptoethanol, reprobed overnight for BDNF staining (ab6201, Abcam, Cambridge, UK), stripped again reprobed for VP16 (ab4808, Abcam, Cambridge, UK), washed and probed for actin (ab179467, Abcam, Cambridge, UK)

Immunohistochemistry

Immunohistochemistry procedure was done as previously described *Lanshakov et al. (2016)*, *Lanshakov et al. (2021)*). After lentivirus infusion on P1 (LV-Syn,n = 2, 18 sections per animal), rat pups were deeply anesthetized with Avertin and transcardially perfused with 1xPBS followed by 1xPBS buffered 4% PFA on P8. The brains were postfixed for 4 hours in 1x PBS buffered with 4% PFA. Then cryoprotected first in 15% sucrose in 1xPBS overnight followed by incubated in 30% sucrose overnight. According to the Neonatal Rat Brain Atlas (*Khazipov et al., 2015*), 25 μm frozen tissue sections were prepared around the mPFC region using the MICROM350 cryostat. Sections were placed on SuperFrost Plus slides (Thermo Fisher Scientific, Waltham, MA, USA). Sections were washed in 1xPBST 0.2% Triton X-100. Blocking was performed with Sea Block (37527, Thermo Fisher Scientific, Waltham, MA, USA) for 1 hour at RT. Sections were then incubated overnight at 4 °C with primary antibodies: rabbit anti-IBA1 (ab178846, Abcam, Cambridge, UK) or rabbit anti-GFAP (Z0334, Dako), and mouse anti-SATB2 (sc-81376, Santa-Cruz), all diluted 1:200 in Sea Block (37527, Thermo Fisher Scientific, Waltham, MA, USA). The next day, sections were washed three times for 15 minutes in 1xPBST. Sections were then incubated with F(ab)2 donkey anti-rabbit Alexa 647 (Jackson Immunoresearch, West Grove, PA, USA), and F(ab)2 donkey anti-mouse Cy3 (Jackson Immunoresearch, West Grove, PA, USA) secondary antibodies diluted 1:500 in Sea Block for 1 hour at room temperature. The slides were then washed three times for 10 minutes each time in 1x PBST. Coverslips

were mounted with Mowiol 4-88 (81381, Sigma Aldrich, St. Louis, MO, USA) containing nuclear counterstain DAPI. Confocal laser scanning microscopy (CLSM, Zeiss LSM 510) was used to analyze the sections. The following laser lines were used for CLSM imaging: DAPI–405 nm, Alexa 488–488 nm, Cy3–543 nm, Alexa 647–633. A tile-scan function (Plan-Apochromat 20x/0.8 M27 objective and 200 μm pinhole) was used to generate panoramic images of the mPFC region. The number of double and triple positive cells was evaluated using the open source software QuPath. Briefly, the EGFP channel was used to detect and mask cells. An appropriate classifier was then created for each channel based on the mean cytoplasmic signal of the detected cells for IBA1 and GFAP or the mean nuclear signal for SATB2 (Santa Cruz). QuPath's definition of double positives is cells that meet the requirements of two classifiers. See the QuPath documentation for a detailed description (*QuPath, 2024*).

Animal experimental design

For the temporal expression increase of different BDNF forms specifically in neurons of the neonatal mPFC, all were cloned in a TET-on lentiviral construct (Fig. 1A). The furin cleavage site was replaced by 4 alanines (126RVRR129 → -126AAAA129). This mutant form (LV-proBDNF_mut) could not be processed by cell proteases. The mature form of BDNF (LV-BDNF) was cloned without the propeptide coding portion. ProBDNF (LV-proBDNF) had no changes except for the C-terminal tag. All forms of BDNF had an HA tag at the C-terminus. At P1 (Fig. 1B), lentiviral particles were infused. The elevated expression of BDNF forms was done from P3 to P8 with a daily subcutaneous injection of DOX 0.2 mg/kg in 100 μl saline. The pups were then returned to their mothers (eight pups per cage, 12 animals per group for behavioral assay, three animals per group for RNAseq) in the home cage and kept intact until P30 for behavioral testing. Animals were then euthanized with CO_2. A portion of the animals were sacrificed at P8 (three animals per group) for transcriptomic study.

Lentivirus production

Lentiviruses were produced in HEK293FT cells (R70007, Thermo), PEG-precipitated, chromatographically purified on quaternary ammonium columns according to *Shaburova & Lanshakov (2021)*. qPCR was used to determine lentiviral titers. Only the 10^9 titer preparation was injected into the mPFC.

Stereotaxic lentivirus injection to rat P1 mPFC

According to R.Z. Khazipov's Neonatal Rat Stereotaxic Atlas (*Khazipov et al., 2015*), lentiviral particles were stereotaxically infused into P1 rat pups. At P1, rat pups were anesthetized with ice cold. They were placed in ice for 5 minutes wrapped in a glove. Hypothermia was chosen because there was less bleeding after the infusion. The pups were then placed in rat stereotaxic apparatus with neonatal adaptors (J & K Seiko, China). One microliter of virus was infused into both hemispheres for 7 minutes using a 10 μl Neuros syringe (Hamilton, Reno, NV, USA) and a 30Ga needle (Hamilton) and a precision syringe pump(LongerPump, China) according to the following coordinates: AP +1.6 mm, ML +0.8 mm, DV +2 mm. After infusion, the needle was left in place for another 7 minutes.
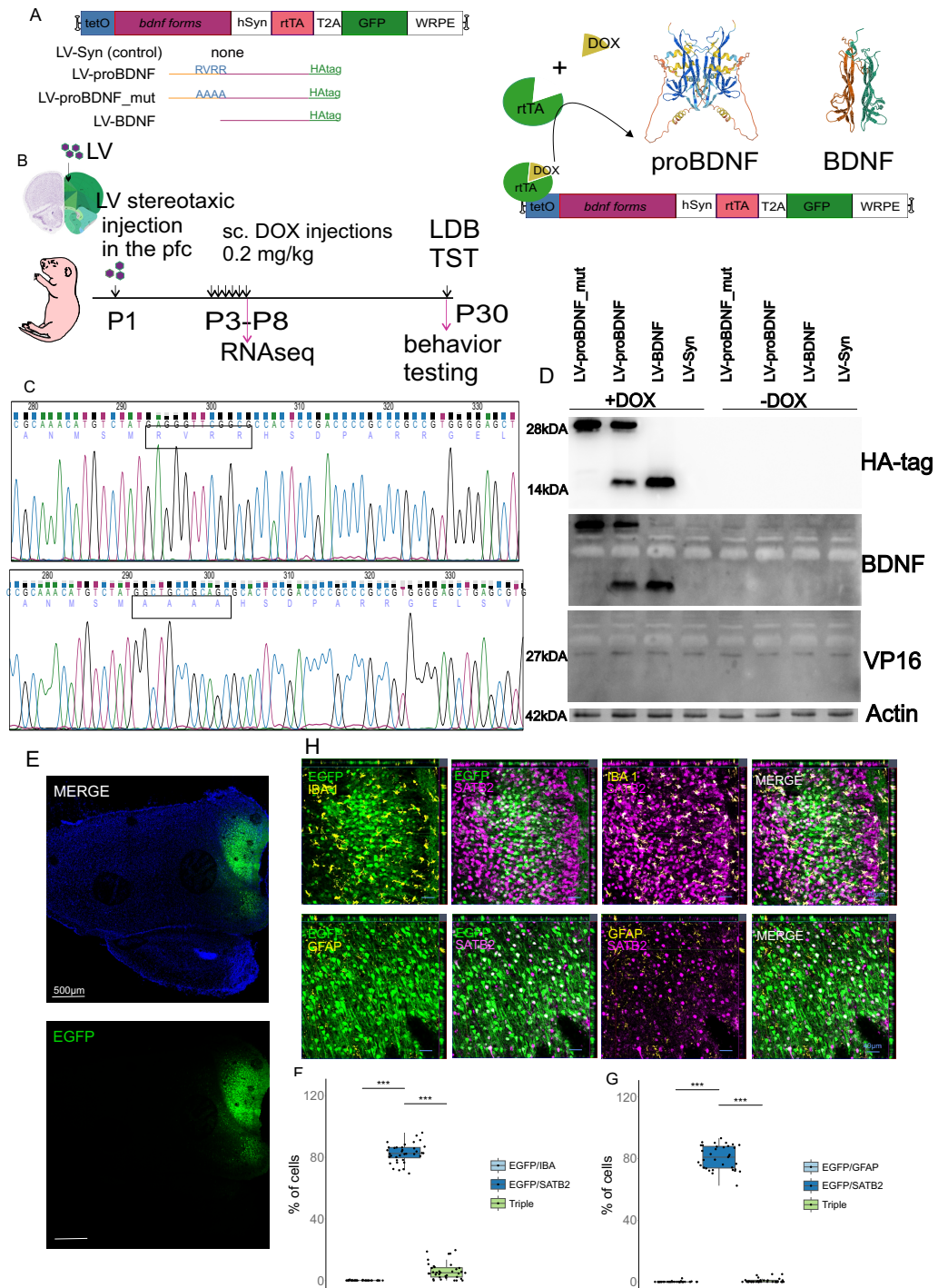
Figure 1 **Experiments main scheme.** (A) Diagram of TET-ON Lentivirus (LV) constructs. (B) LV particles were injected into the mPFC area on P1. DOX for expression induction was injected subcutaneously on P3-P8 and behavioral testing was performed on P30. (C) Sequenogram of the cleavage site in proBDNF and mutant constructs (D) Representative Western blot image showing induction of construct expression in CHO-K1 cells. (E) Panoramic CLSM image of the P8 rat pup brain after LV-Syn injection on P1 (F) Results of immunohistochemical quantification SATB2/GFAP double immunohistochemistry (G) Results of immunohistochemical quantification SATB2/IBA1 double immunohistochemistry (H) Representative higher magnification microscopic images of mPFC (orthoprojections).

Full-size 🖼 DOI: 10.7717/peerj.18465/fig-1

A 30Ga Hamilton needle was used. The puncture was made directly to the head. After surgery, 100 µl of 100 µg/mL penicillin and 100 µg/mL streptomycin solution in 1xPBS were injected intraperitoneally. The pups were then recovered on the warming pad and returned to the mother.

Behavior testing

At P30, anxiety-like behavior was assessed using the light-dark box (LDB) test. Rats were tested in the (30 cm × 60 cm × 30 cm) halved into two compartments: light and dark (30 cm × 30 cm × 30 cm). All the walls in each part were either white or black. The partition connecting two compartments had an opening of 6.5 cm × 6.5 cm. The light in the room was dimmed. A small 5W gooseneck lamp with a clamp was mounted above the light compartment, providing light (600 lux) to the center of the box. Illumination in the dark compartment was 5 lux (*Narayanan & Kumar, 2018*). Digital camera captures video above the device. Animals were placed in the light compartment facing the door between compartments. The duration of the test was 5 minutes. After each animal, the apparatus was cleaned with 70% ethanol and allowed to dry before the next subject was tested. After testing, the animals were placed in a separate cage and returned to the home cage when all animals in that cage had been tested. In the LDB test, the time in the white field, the number of complete transitions, and the number of stretches from the dark field to the white field were counted on videotapes by three independent observers. One week after the first test, depressive-like behavior was assessed with the Tail Suspension Test (TST) (*Can et al., 2011*). The animals were suspended 60 cm off the ground with paper tape over medical tape attached to a rat's tail. Apparatus were isolated from sides and back. Test lasted 5 minutes as LDB. After each animal, the arena was cleaned with 70% ethanol. After the test, the animals were placed in a separate cage and returned to the home cage when all animals in that cage were tested as above. In the TST, total immobile time, active time, and latency were counted by three independent observers.

Statistics

Statistical analyses were performed with R. For the behavioral analysis, linear mixed effects models (nlme package (*José C. Pinheiro, 2000*)) were used with lentiviral injection group as a fixed effect and animal ID as a random effect. Mixed models are often preferred to traditional analysis of variance and regression models because of their flexibility in dealing with missing values and uneven distribution of a random variable (*Yang et al., 2014*). Means were compared by Tukey test, emmeans R package (*Searle, Speed & Milliken, 1980*). Normality was tested using the Shapiro–Wilk test. Data of time spent in the white compartment were Boxcox transformed (*Daimon, 2011*). Immunohistochemistry data were analyzed using the non-parametric Mann–Whitney test.

mPFC samples collection and RNA extraction

Pups were sacrificed by rapid decapitation with scissors one hour after the last DOX injection at P8. There were three animals per group for the RNAseq experiments. To enrich RNA samples for neuronal transcripts, mPFC was dissected under a binocular microscope and the pia was removed. The samples were then immediately weighted. The total weight

of each mPFC sample did not exceed 26 mg. RNA was isolated using the Norgen Total RNA Purification Kit according to the manufacturer's protocol. RNA samples were treated on columns with RNAse-free DNAse I (Sigma Aldrich). After elution, 40 U of ribonuclease inhibitor Ribolock (Thermo) was added to the samples.

RNA-sequencing

RNA samples were used to prepare cDNA libraries using the QIAseq Stranded Total RNA Lib Kit (Qiagen, Hilden, Germany) according to the manufacturer's protocol. Ribosomal RNA depletion was performed with NEBNext rRNA Depletion Kit (New England Biolabs Inc., Ipswich, MA, USA). The concentration of cDNA libraries was measured by the dsDNA High Sensitivity Kit on a Qubit 4.0 fluorometer (Thermo Fisher Scientific). The quality of cDNA libraries was assessed using High Sensitivity D1000 ScreenTape on a 4150 TapeStation (Agilent). Libraries were sequenced on a NextSeq instrument (Illumina) using single-end 75 bp reads, 15M reads per sample. Each experimental point was biological replicate. The statistical power of this experimental design, calculated in RNASeqPower is 0.8. Adapter sequences were cut with Trimmomatic (*Bolger, Lohse & Usadel, 2014*). Raw reads were aligned to the mRn7.2 reference genome using Hisat2 (*Kim, Langmead & Salzberg, 2015*). The number of mapped reads was counted by the Rsubread (*Liao, Smyth & Shi, 2019*). The edger package (*McCarthy, Chen & Smyth, 2012*) was used to detect DEGs between LV-BDNF *vs* LV-Syn; LV-proBDNF *vs* LV-Syn; LV-proBDNF_mut *vs* LV-Syn. Edger's default Trimmed Mean of M (TMM) method was used to normalize the libraries. Edger's Generalized Linear Models (GLM) approach was used to identify the DEGs.

Functional annotation

Functional annotation of differentially expressed genes was performed using the R clusterprofile package (*Wu et al., 2021*). DEGs with $|log2FC| > 1$ and $p < 0.05$ have been selected.

snRNAseq data

Single-nucleus RNAseq data from neonatal rat cortex were obtained from the control samples of the *Chen et al. (2022)* study (NCBI GEO: GSE185538). The Seurat 4.3.0 package was used to analyze the gene expression of cell clusters (*Hao et al., 2021*)
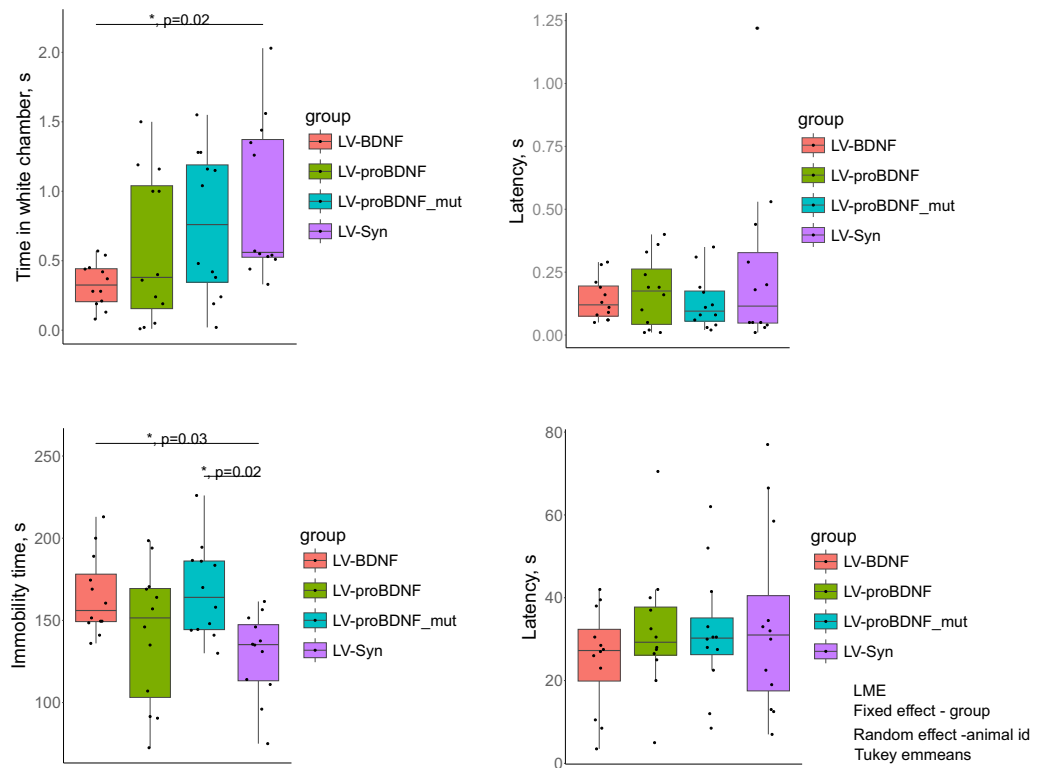
RESULTS

Proof of constructs

Based on Dr. Adam Karpf's plasmid, we have constructed an all-in-one TET-ON lentiviral construct for transgene expression induction with DOX in neurons. Sequences encoding pro-, mature and mutant *Bdnf* with HA tag were then placed under the tight-TRE promoter (Fig. 1A) and verified by Sanger sequencing (Fig. 1C). After stereotaxic lentiviral infusion to P1 male rat mPFC expression was induced for 6 consecutive days from P3 to P8 (Fig. 1B) for the main experiment. See the Methods section for a detailed description. For the initial evaluation of the construct, we performed preliminary experiments with transfection of CHO-K1 cells and Western blotting. These experiments showed the absence of protein

products without DOX and the presence of all expected forms 14kDA for mature BDNF and 28kDA for proBDNF and proBDNF_mut with anti-HA tag antibodies when DOX was added to the cell culture medium (Fig. 1D, original Western blot photos are in the Supplementary Material). After stripping, the membrane was reprobed with anti-BDNF antibody. Bands corresponding to proBDNF were present in all lines. After another round of stripping, the membrane was probed for VP16, which is present in rtTA. All lines had corresponding bands. We then checked which cells in the neonatal mPFC we could see expressing the EGFP reporter. Stereotaxically infused control LV-Syn lentivirus on P1, we looked at reporter expression and injection site placement on P8 to fit the scheme of this experiment with the main RNA-seq experiment. Panoramic confocal images show that with the chosen stereotaxic coordinates we obtained reporter expression in the mPFC (Fig. 1E). Double immunohistochemistry with callosal neuron marker SATB2 and mikroglial marker IBA1 using EGFP fluorescence showed that approximately 80% (95% CI [80.5–84.7]) of EGFP-positive cells were SATB2-positive and only 0.03% (95% CI [−0.0123–0.0679]) were IBA1-positive (p.adj(BH) < 0.01, Mann-Whitney U test, Figs. 1F, 1H. A slightly increased 6.19% (95% CI [4.35–8.03]) number of triple positive cells was observed. This could be explained by the expression of SATB1 in the immune cells and weak antibody cross-reactivity (*Burute, Gottimukkala & Galande, 2012*). Double immunohistochemistry with SATB2 and the astrocyte marker GFAP again showed about 80% EGFP/SATB2 positive cells (96% CI [78.0–83.3]) and almost no double EGFP/GFAP 0.1% (95% CI [−0.0344–0.234]) and triple positives 0.694% (95% CI [0.221–1.17]; p.adj(BH) < 0.01, Mann-Whitney U test, Figs. 1G, 1H). This means that most of the transduced cells were neurons.

Increased expression of different forms of BDNF in the mPFC in the neonatal period has an effect on anxiety and depressive-like behavior in the adolescent period

Temporary increase in expression of mature BDNF (LV-BDNF) in the mPFC had a significant effect on anxiety (Fig. 2). Induction of LV-BDNF expression in the neonatal period had an anxiogenic effect in adolescence. These animals spent significantly less time in the white compartment ($p = 0.02$, AIC $= −33.12748$ BIC $= −21.90027$) compared to the control LV-Syn. No significant changes in anxiety were observed after expression induction of other constructs. The latency to enter the dark compartment was also not significantly changed in any group. There were no significant differences between groups for other parameters. We were also surprised by changes in depressive-like behavior. The immobility time in the tail suspension test was significantly higher in the LV-BDNF group with induction of mature BDNF expression at P3-P8 ($p = 0.0327$, AIC $= 473.5392$, BIC $= 484.7664$) compared to the LV-Syn control. Increased expression of the mutant form of LV-proBDNF_mut also caused an increase in immobility time ($p = 0.02472$) (Fig. 2) compared to control LV-Syn. Latency to immobility did not change between groups. Thus, we could conclude that increased expression of the mature form of BDNF in the neonatal mPFC is involved in increased anxiety and depressive-like behavior in adolescence. Expression of the mutant form has the same effect, but only on depressive-like behavior.

**Figure 2 Behavior changes at P30.** Upper graph row - LDB test results, lower row - TST results.

Full-size 🖼 DOI: 10.7717/peerj.18465/fig-2

Transcriptomic changes at P8 following lentiviral expression induction

We saw behavioral effects only after activation of LV-BDNF and LV-proBDNF_mut expression, but the transcriptome was altered in each group. In the PCA plot, the distribution of experimental points in the PCA dimensions depends on the observed total transcriptomic changes (Fig. 3). Interestingly, experimental points of animals with proform expression (LV-proBDNF, LV-proBDNF_mut) were closer to controls (LV-Syn, (Fig. 3)), more distinct points were with expression of mature BDNF. The volcano plots show that genes that are upregulated in the LV-BDNF group are downregulated in LV-proBDNF_mut or LV-proBDNF. These genes are *Ptgds, Fam180a, Itgb4, Ranbp3l, Bnc2, Slc6a13, Slc22a6* (Fig. 4, Table S1). There were also genes that were present in all three DEG lists after viral injections. They were *Ptprh*, which was upregulated, and *Ifitm3*, which was downregulated. Amount of common genes represented on a Venn diagram.

Functional annotation of differentially expressed genes

Surprisingly, GO enrichment analysis yielded more terms only after LV-BDNF and far fewer terms after LV-proBDNF and LV-proBDNF_mut (Fig. 5). After BDNF expression induction were enriched such terms-"bone development", "endochondral bone morphogenesis", "bone morphogenesis", "cartilage development", "ossification", "response to retinoic acid", "extracellular matrix organization", "response to estradiol",

Lanshakov et al. (2024), *PeerJ*, DOI 10.7717/peerj.18465

11/29
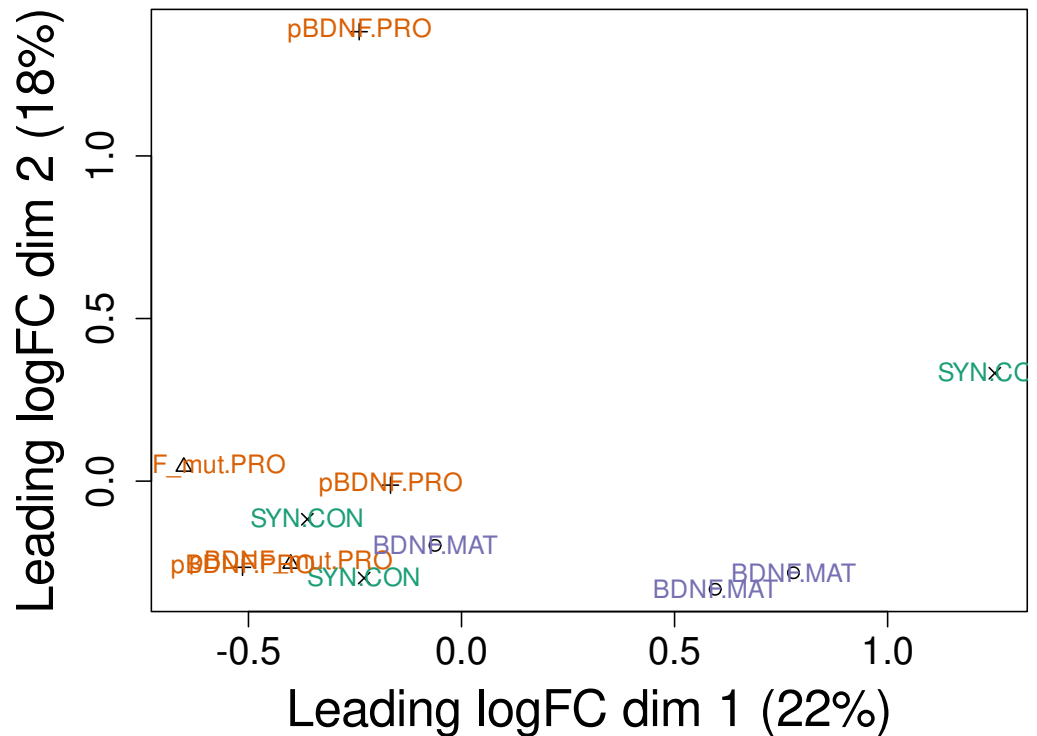
Figure 3 RNAseq experimental points displayed in principal component analysis (PCA) dimensions and variability described by these components.

"positive regulation of hormone biosynthesis process", "transforming growth factor beta 1 production". After LV-proBDNF, "rough endoplasmic reticulum", "basolateral plasma membrane", "nuclear membrane", "nuclear envelope lumen", "outer dense fiber" were enriched. After LV-proBDNF_mut, the list of terms was completely different: "extracellular matrix structural component conferring tensile strength", "extracellular matrix structural component", "SMAD binding", "rDNA binding", "phospholipase A1 activity", "oxidoreductase activity, acting on NAD(P)H, heme protein as acceptor", "co-SMAD binding". If we look at the cnetplots (Fig. 5) of the enriched terms and the related genes that fulfill these terms after each viral injection, it is mostly the genes mentioned above (*Bnc2, Ptgds, Rnabp3l, Slc6a13, Slc22a6, Slc13a4, Tgif1*) and shown in the second column of plots in the figure. *Rarb, Igf2, Bmp6, Penk, Clec3b, Aldh1a2, Slc13a4* were upregulated only after LV-BDNF. *Slc6a13, Slc22a6* from the term "basolateral plasma membrane" were upregulated after LV-BDNF and downregulated after proBDNF.

Neonatal neocortex sn-RNAseq

We took only control samples from Chen's study (*Chen et al., 2022*). The analysis in the Seurat package revealed a slightly larger number of cell types. However, the overall picture
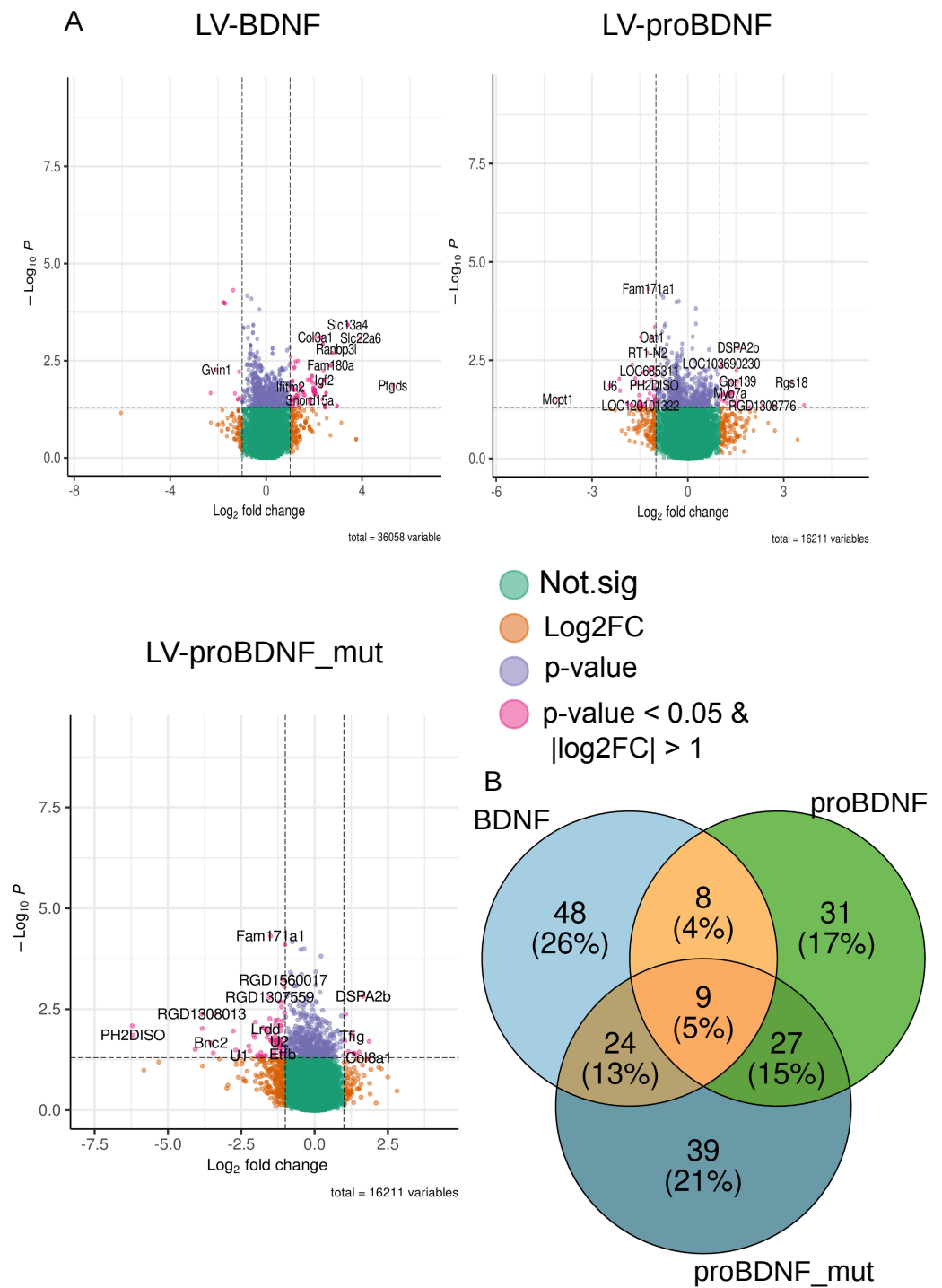
Figure 4 (A) **Volcano plots of selected DEGs after each LV injection and expression induction.** Genes with $|log2FC| > 1$ and $p < 0.05$ were selected. (B) Venn diagram of common genes of DEGs.

Full-size 🖼 DOI: 10.7717/peerj.18465/fig-4
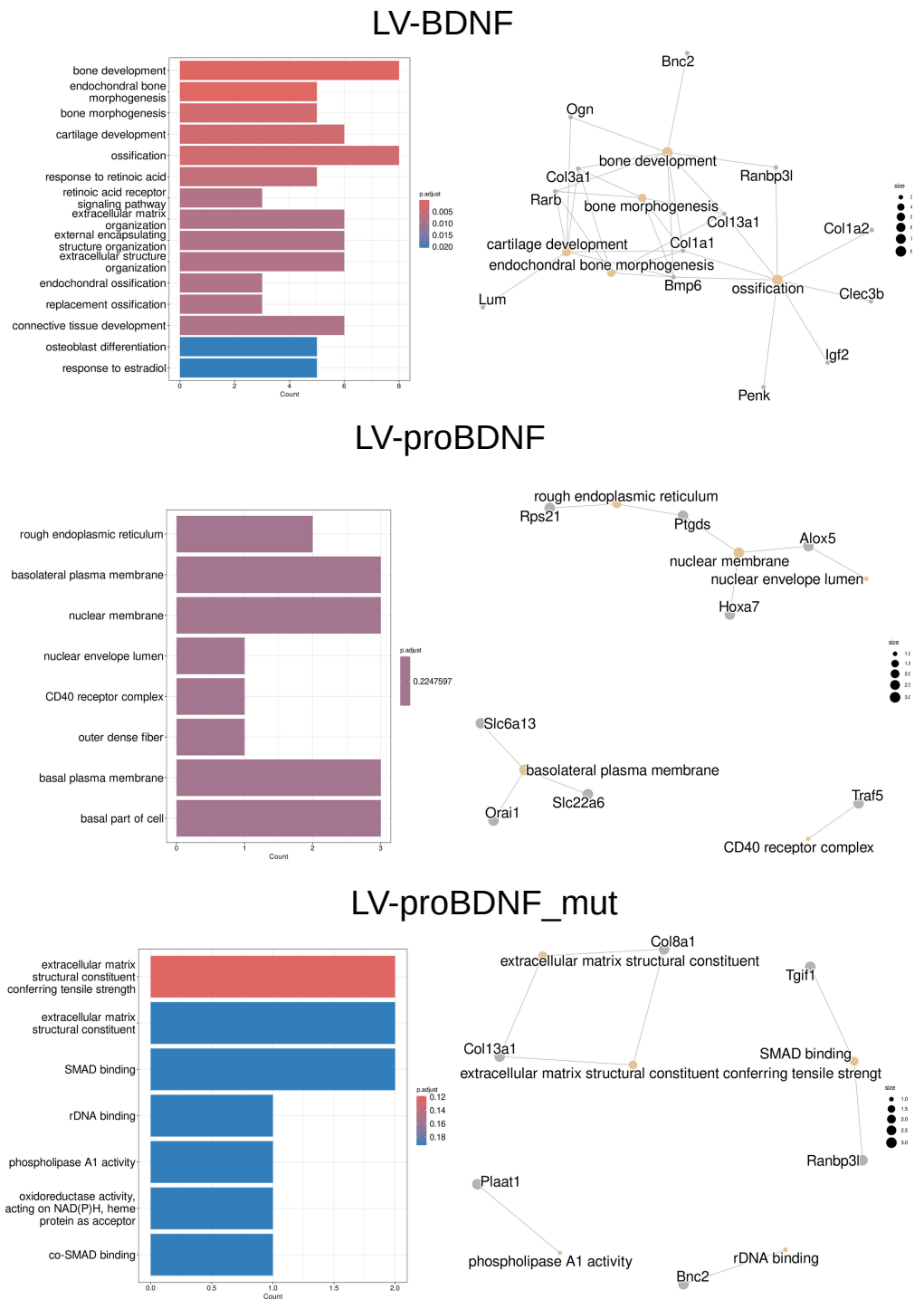
Figure 5 Enrichment analysis of DEGs on the basis of clusterProfiler packages. Major biological processes GO terms of $|log\,2FC| > 1$ - left panel. Gene concept network (cnetplot) of the most enriched BP GO terms and the overlapping set of genes consisting of these terms after each LV injection - right panel.

Full-size 🔜 DOI: 10.7717/peerj.18465/fig-5
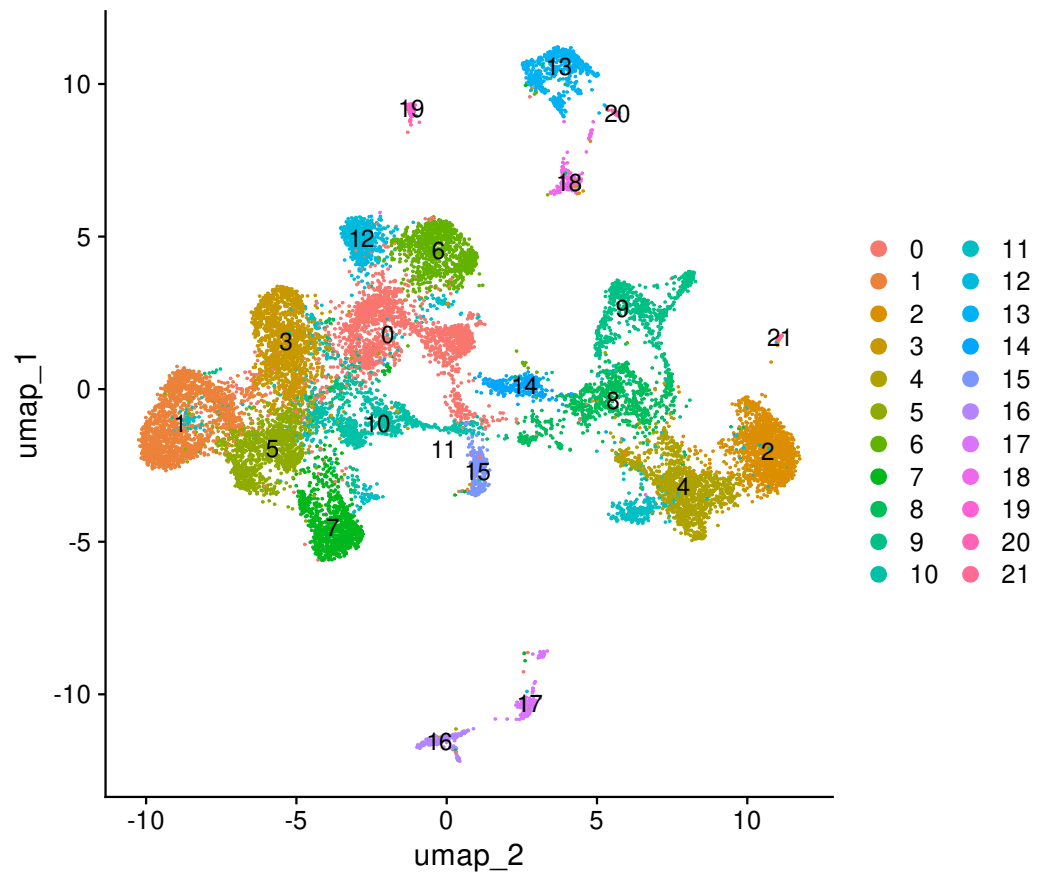
Figure 6 Results of snRNAseq data analysis and clustering of cells.

Full-size 🖼 DOI: 10.7717/peerj.18465/fig-6

remains the same (Fig. 6) Slightly different parameters selected for clustering could explain additional cell cluster.

Interestingly, there are three types of astroglial cells in the rat neonatal cortex, and only one of them expresses GFAP. Cells of two other astroglial clusters express *Aqp4* and *Slc1a2* (Fig. 7). Although it is not correlated for the present study, we consider this fact very important for developmental neuroscience, together with the consistency validation of our analysis of snRNAseq data.

Cell specificity of DEG expression

Analysis of selected DEGs described above in the context of rat neonatal cortex cell types revealed that these genes are predominantly expressed in clusters 16 and 17. It could be seen on the feature plots of the selected genes (Fig. 8). The list of genes that are exclusive markers for these clusters is shown in Tables S2–S3. In cluster 16, the perivascular stromal cells (PSC), *Col1a1, Bnc2* are expressed. Cluster 17 consists of pericytes (PC) that express *Pdgfrb, Vtn, Ptgds* (Tables S2–S3, Figs. S2–S3). As mentioned above, in these (PSC, PC) cell types, the expression of mature BDNF caused an increase in the expression of marker genes. Expression of proBDNF and its mutant form decreased the mRNA level of these
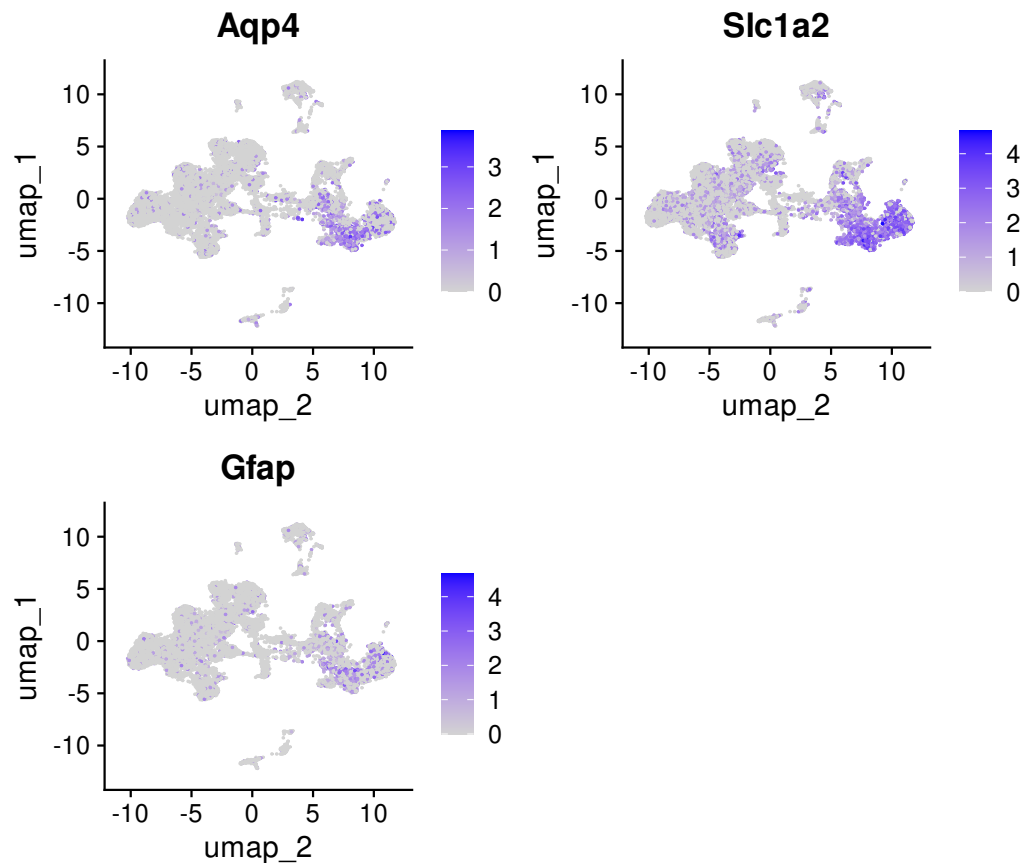
Figure 7 **FeaturePlots showing the expression of selected genes *Aqp4, Slc1a2, Gfap* in three classes of astrocytes in neonatal rat brain.** logFC scale shown in purple.

genes. This means that after expression activation, the main transcriptional response was observed in PSC and PC.

Predominantly neuronal and glial genes altered after expression induction

As shown earlier, we have seen mostly transcriptional responses from PSC and PC cells. It was opposite depending on mature or proform expression induction. At the same time, changes in anxiety and depressive-like behaviors were the same. To further elucidate the molecular mechanism underlying these processes, we searched the DEG lists for genes that are predominantly expressed in neurons and glial cells (Fig. 9). After LV-BDNF we should note *Naaladl2* log2FC = 1, *Ifitm2* log2FC = 1, *Atp5mk* log2FC = −1.72, *Rarb* log2FC = 1.5, *Fam171a1* log2FC = −1.37, *Tgif1* log2FC = 1.43, *Nmi* log2FC = 1.11, *Penk* log2FC = 1.25. After LV-proBDNF *Styk1* log2FC = 1.4, *Rps21* log2FC = −1.03, *Nr4a2* log2FC = 2.62, *Tex47* log2FC = −1, *Orai1* log2FC = 1.13, *Fam171a1* log2FC = −1.23, *Rsph1* log2FC = −1.03, *Zfp52* log2FC = 1.03, *Susd2* log2FC = 1.23, *Pnpla1* log2FC = −1.03, *Fcgr3a* log2FC = 1.23, *Tmco4* log2FC = −1.65, *Traf5* log2FC = 1.33 were changed. After LV-proBDNF_mut *Snrpf* log2FC = −1.13, *Etfb* log2FC = −1.09, *Dll3* log2FC = −1.17,
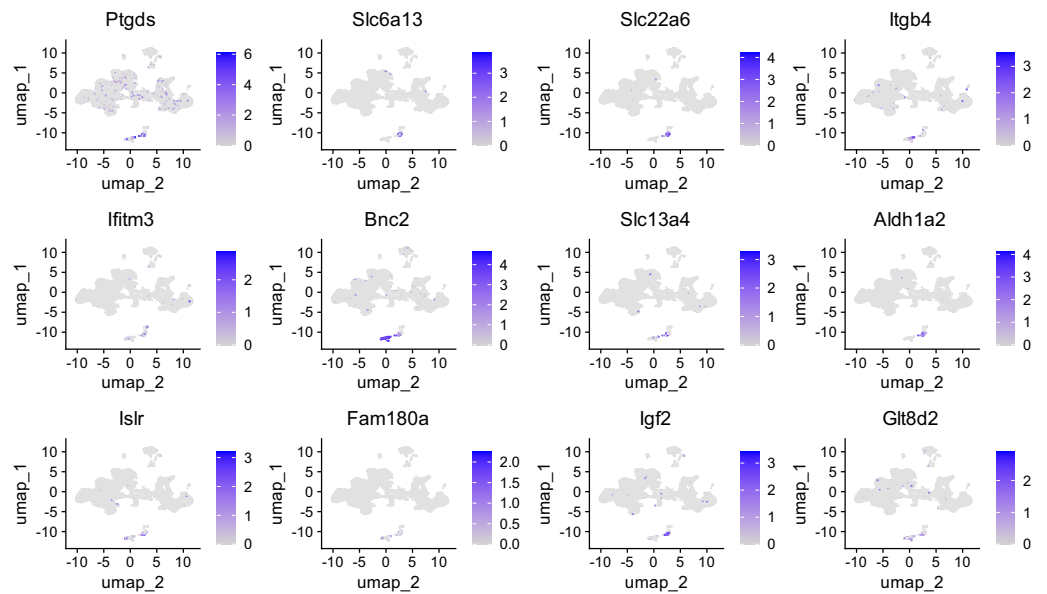
Figure 8 FeaturePlots showing the expression of selected genes that were mainly changed after BDNF expression induction across cell clusters. logFC scale shown in purple.
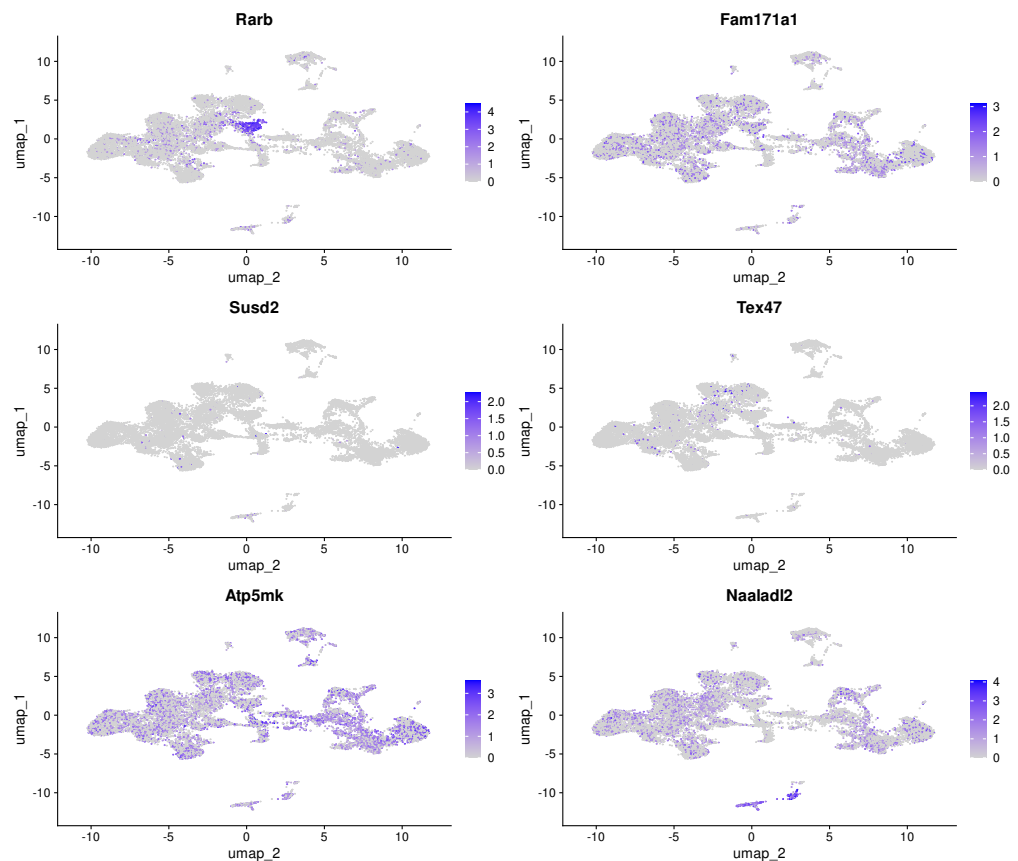
Full-size 🖼 DOI: 10.7717/peerj.18465/fig-8

Tex47 log2FC = −1.09, *Rbm46* log2FC = −1.16, *RGD1359290* log2FC = −1.01, *Sim2* log2FC = −1.06, Susd2 log2FC = 1.33, Grm4 log2FC = 1.03, Fa2 h log2FC = −1.49, Gadd45b log2FC = −1.11, Fam171a1 log2FC = −1.5. All these genes are mainly expressed in different neuronal and glial cell types, with the exception of *Fcgr3a*, which is expressed in microglia. After all three LV injections, *Fam171a1* was downregulated. After Proforms expression induction, *Susd2* and *Tex47* changed in a co-directional way. The other genes were exclusive to each LV.

DISCUSSION

Temporally increased expression of pro-, mature-, and unprocessed (mutant) BDNF forms in the neonatal mPFC had an effect on anxiety and depressive-like behaviors in adolescence. We expected an anxiolytic and antidepressant effect. Instead, we got the opposite. Expression of mature BDNF increased indicators of anxiety and depressive-like behavior in the tests, expression of mutant BDNF (proBDNF_mut) increased only depressive-like behavior. Behavior was not affected by expression of proBDNF.

Mature BDNF is known to improve memory and cognition through TrkB receptors (*Cunha, Brambilla & Thomas, 2010*; *Miranda et al., 2019*). Individuals with higher cognitive abilities have higher demands on environmental conditions. Therefore, increased anxiety and depressive-like behavior may be related to our observations. To summarize, we can say that people with a higher IQ tend to be predisposed to anxiety and depression (*Melby et al., 2020*). Our findings are also supported by the fact that mice lacking *Trkbt1*, with increased mature BDNF signaling, showed increased anxiety (*Watson et al., 2015*). To determine which gene expression changes in the mPFC at P8 are responsible for behavioral

Figure 9 **FeaturePlots showing mainly neuronal and glial genes that were affected after BDNF expression induction.** logFC scale shown in purple.

Full-size ◨ DOI: 10.7717/peerj.18465/fig-9

changes, we performed RNA-seq analysis of mPFC samples. Surprisingly, we saw the main transcriptional response in PSC and PC cells. Perivascular stromal cells in the brain are a heterogeneous population of cells associated with the vasculature, including endothelial cells, pericytes, and astrocytes. These cells contribute significantly to the structure, function, and integrity of the blood-brain barrier (BBB) and are involved in various processes such as vascular architecture, scavenging and immunoregulatory functions (*Kida et al., 1993*), maturation, and neuroinflammation, mesenchymal and neuroectodermal differentiation potential (*Paul et al., 2012*; *Lojewski et al., 2015*). Brain pericytes are multifunctional cells located on the abluminal side of the capillaries throughout the brain, playing pivotal roles in the maintenance and function of the neurovascular unit(NVU) (*Brown et al., 2019*). These cells are crucial for the development and integrity of the blood-brain barrier (BBB), regulation of cerebral blood flow, vascular development and angiogenesis, neuroinflammation management (*Rustenhoven et al., 2017*), and even stem cell-like activities (*Dore-Duffy, 2008*).

The observed transcriptional response was inversely dependent on the form of BDNF, with marker gene expression upregulation after mature BDNF and downregulation after

proforms. We could not conclude that this expression reflected changes in the amount of a particular cell type. Detailed immunohistochemical studies using cell type antibody markers are required to make such a conclusion.

Notable genes that behave in this way are *Bnc-2* Basonuclin 2 (PSC) and *Ptgds* Prostaglandin D2 Synthase (PC). *Ptgds* is highly expressed in the PC then in the PSC log2FC 5.5 *vs.* 2.78. Some weak expression is detected in neuronal and glial cells (Fig. 8). It has been shown that in patients with rapid-cycling bipolar disorder, *Ptgds* mRNA levels are reduced in peripheral blood mononuclear cells. Prostaglandin D2 synthase (PTGDS) is an enzyme that catalyzes the conversion of prostaglandin H2 (PGH2) to prostaglandin D2 (PGD2). PGH2 is a common precursor for various prostaglandins, which are lipid compounds that participate in a wide range of body functions including inflammation, pain, and fever responses, as well as the regulation of blood pressure and coagulation. PTGDS specifically takes PGH2 and converts it into PGD2, a prostaglandin involved in several important physiological processes: sleep regulation (*Pahl, 2007*), inflammation and immune response (*Rajakariar et al., 2007*), allergic reactions (*García-Solaesa et al., 2014*), vasodilation and blood pressure regulation (*Mohri et al., 2007*), platelet aggregation. PGD2 is a major prostaglandin produced in the central nervous system and is involved in the regulation of sleep and pain responses through DP receptors. It acts as a sleep-promoting substance (*Pahl, 2007*).

In the immune cells prostaglandin D2 synthase (hPGD2S) metabolizes cyclooxygenase (COX)-derived PGH2 to PGD2 and 15-deoxy δ12–14 PGJ2. PGD2 plays crucial roles in the control of inflammation, where it can act as both a pro- and anti-inflammatory mediator (*Rajakariar et al., 2007*). PGD2's role in vasodilation and the regulation of blood pressure is significant, illustrating the compound's effect on vascular diameter and cardiovascular health. This function is critical for maintaining vascular homeostasis (*Mohri et al., 2007*). Genome-wide association study of sporadic brain arteriovenous malformations showed *Bnc2* intron SNP association with nominal $p < 0.1$ (*Weinsheimer et al., 2016*). Experiments on BV2 cell lines suggest that circular RNA Circ-*Bnc2* alleviates neuroinflammation in LPS-stimulated microglial cells through regulating miR-497a-5p/HECTD1 axis (*Chen & Cao, 2023*). Circular RNAs (circRNAs) like circ-*Bnc2* are generated from pre-mRNA back-splicing, where a downstream splice donor site is joined to an upstream splice acceptor site. This process leads to the production of a covalently closed loop structure without 5′ to 3′ polarity and a polyadenylated tail, distinguishing them from linear RNA counterparts.

Slc6a13, Slc22a6, Slc13a4 is another set of genes that should be noted. These genes consist of the solute carrier family. While *Slc6a13* shares the solute carrier family designation with *Slc6a1*, indicating it's part of the broader family of membrane transport proteins that play crucial roles in neurotransmitter regulation, the specific details regarding *Slc6a13* and its link to neuropsychiatric disorders are uncertain. *Slc6a13* is known to encode a GABA transporter, suggesting its importance in GABAergic signaling pathways similar to *Slc6a1* (*Bhatt et al., 2023*). The *Slc6a1* gene has been linked to various neurodevelopmental disorders (*Goodspeed et al., 2023*), including epilepsy (*Johannesen et al., 2023*), intellectual disability(ID), and autistic spectrum disorders (ASD), among others. The gene encodes for the GABA transporter 1 (*Gat-1*), which is responsible for the reuptake of GABA from

the synaptic cleft, playing a crucial role in maintaining neurotransmitter homeostasis and modulating neurotransmission. Abnormalities in *Gat-1* function due to *Slc6a1* variants can disrupt GABAergic signaling, contributing to the pathogenesis of these disorders.

Slc22a6, known as the organic anion transporter 1 (OAT1), is part of the SLC22 family, which includes organic cation transporters (OCTs), organic anion transporters (OATs), and organic zwitterion/cation transporters(OCTNs) (*Parker et al., 2023*) . This family plays a crucial role in regulating the cellular uptake and excretion of various endogenous and exogenous substances, including metabolic by-products, toxins, and pharmaceuticals. While primarily recognized for their roles in the kidneys and liver, members of the SLC22 family also have significant functions in the brain, contributing to homeostasis and the detoxification of harmful substances. *Slc13a4* is recognized for its role in transporting nutrient sulfate across the placenta to the fetus, which is crucial for human development (*Rakoczy et al., 2015*) However, its specific function in the brain is not well-documented in the studies available. It was shown that expression levels for the sulfate transporter *Slc13a4* to be elevated during postnatal development, and sulfate accumulation in the brains of *Slc13a4* +/- mice is reduced, suggesting a role for this transporter during this critical window of brain development (*Harvey et al., 2021*).

Observed similar behavioral changes after mature and pro-form expression induction led us to look deeper beyond the transcriptional response in PSC and PC cells. Genes primarily expressed in neurons and glial cells were differentially altered after each LV, except for *Fam171a1*, *Susd2* and *Tex47*. *Fam171a1*, Astroprincin (*Apcn*) is a recently characterized transmembrane glycoprotein that is abundant in brain astrocytes and is overexpressed in some tumors (*Wahab et al., 2020*). However, detailed functional roles and mechanisms of *Apcn* in the brain and its contribution to diseases, including its overexpression in tumors, are still being elucidated. Astroprincin's identification as abundant in astrocytes hints at its potential involvement in neurobiological processes and astrocyte functions. Astrocytes play crucial roles in maintaining the homeostasis of the central nervous system (CNS), including neurotransmitter uptake and recycling, providing metabolic support to neurons, contributing to the blood-brain barrier's integrity, and participating in the brain's response to injury. *Susd2* regulates neurite outgrowth and synaptic density in hippocampal cultures. It is a transmembrane protein with a complement control protein (CCP) domain, previously identified as a tumor-reversing protein but without a characterized function in the CNS. *Susd2* expression peaks two weeks after birth, coinciding with synaptogenesis (*Nadjar et al., 2015*). It localizes to soma, axons, dendrites, and associates with excitatory synapses. Inhibition of *Susd2* reduces the number of excitatory synaptic profiles and alters morphological parameters, suggesting that it alters adhesion properties and plays a dual role at different stages of development. There is not much information about *Tex47* function in the brain, it has primarily function in reproductive tissues such as the testes, influencing spermatogenesis or other aspects of male fertility..

Another gene of note that has been altered by LV-BDNF is the *Rarb* gene. Retinoic Acid Receptor Beta (RARB) plays a crucial role in various developmental and physiological processes, especially in the brain, mediated by retinoic acid signaling. Research has shown that RARB, along with other retinoic acid receptors, is involved in the molecular patterning

of the PFC and motor areas, the development of reciprocal PFC-mediodorsal thalamus connectivity, and intra-PFC synaptogenesis. These processes are crucial for the proper function and structural development of the PFC, highlighting the importance of retinoic acid signaling in brain development and potentially its evolutionary expansion. Retinoic acid (RA) signaling, mediated through RARB and other receptors, is essential for the molecular patterning of the PFC. This signaling is required for the expression of layer 4 markers, intra-PFC synaptogenesis, and the development of reciprocal connectivity between the PFC and the mediodorsal thalamus. These findings indicate a critical role for RA signaling in the establishment of the structural and functional architecture of the PFC during development (*Shibata et al., 2021*).

CONCLUSIONS

In conclusion, we found that increased expression of mature BDNF (LV-BDNF) at P5-P8 resulted in increased anxiety and depressive-like behaviors at P30. Conversely, expression of a mutant form of BDNF (LV-pBDNF_mut) only increased immobility in the tail suspension test. Using our RNA-seq data and available online single-nucleus RNA sequencing results, we analyzed transcriptomic changes in the neonatal mPFC at P8 that may underlie the observed behavioral changes from a cell type perspective. Expression of matBDNF triggered an enhanced transcriptional response in perivascular stromal cells (PSC) and pericyte cells (PC), particularly affecting genes such as *Ptgds, Slc6a13, Slc22a6, Bnc2, Slc13a4* and *Aldh1a2*. Interestingly, *Ptgds* is identified by GWAS as a candidate gene associated with ADHD and bipolar disorder (*Pujol-Gualdo et al., 2021*; *Marín-Méndez et al., 2012*; *Munkholm et al., 2015*). The observed similar behavioral phenotype after expression of mature and mutant forms of BDNF, together with the detected genes associated with bipolar disorder, supported that *Bdnf* could play a substantial role in the pathogenesis of this neurobehavioral disorder. It is noteworthy that proforms induced transcriptional responses in PSC, PC that were completely opposite to those induced by LV-BDNF. This study underscores the intricate role of BDNF's various forms in the development of the nervous system and their potential long-term impacts on behavior, offering new insights into the neurobiological underpinnings of psychiatric disorders.

ACKNOWLEDGEMENTS

ADDITIONAL INFORMATION AND DECLARATIONS

Competing Interests

The authors declare there are no competing interests.

Author Contributions

- Dmitriy Lanshakov conceived and designed the experiments, performed the experiments, analyzed the data, prepared figures and/or tables, and approved the final draft.
- Elizaveta Shaburova performed the experiments, analyzed the data, authored or reviewed drafts of the article, and approved the final draft.
- Ekaterina Sukhareva performed the experiments, analyzed the data, authored or reviewed drafts of the article, and approved the final draft.
- Veta Bulygina performed the experiments, analyzed the data, authored or reviewed drafts of the article, and approved the final draft.
- Uliana Drozd performed the experiments, analyzed the data, prepared figures and/or tables, and approved the final draft.
- Irina Larionova performed the experiments, analyzed the data, prepared figures and/or tables, and approved the final draft.
- Tatiana Gerashchenko performed the experiments, analyzed the data, prepared figures and/or tables, authored or reviewed drafts of the article, and approved the final draft.
- Tatiana Shnaider performed the experiments, analyzed the data, prepared figures and/or tables, and approved the final draft.
- Evgeny V. Denisov conceived and designed the experiments, analyzed the data, prepared figures and/or tables, and approved the final draft.
- Tatyana Kalinina conceived and designed the experiments, performed the experiments, analyzed the data, prepared figures and/or tables, and approved the final draft.

Animal Ethics

The following information was supplied relating to ethical approvals (i.e., approving body and any reference numbers):

All animal procedures were approved through the Institute of Cytology and Genetics Animal Care and Use Committee (protocol 151 from 28.04.2023)

DNA Deposition

The following information was supplied regarding the deposition of DNA sequences:

The raw reads are available at ENA database: PRJEB47241.

Data Availability

The following information was supplied regarding data availability:

The behavior testing data, Immunohistochemistry data, supplemental figures and raw western blot photos are available in the Supplemental Files and also at Zenodo DOI: Lanshakov, D., Shaburova, E., Sukhareva, E., Bulygina, V., Drozd, U., Larionova, L., Gerashchenko, T., Shnaider, T., Denisov, E., & Kalinina, T. (2024). PeerJ Supplemet 2024 [Data set]. Zenodo. https://doi.org/10.5281/zenodo.13773297.

Supplemental Information

Supplemental information for this article can be found online at http://dx.doi.org/10.7717/peerj.18465#supplemental-information.

REFERENCES

Amiri A, Coppola G, Scuderi S, Wu F, Roychowdhury T, Liu F, Pochareddy S, Shin Y, Safi A, Song L, Zhu Y, Sousa AMM, Gerstein M, Crawford GE, Sestan N, Abyzov A, Vaccarino FM. 2018. Transcriptome and epigenome landscape of human cortical development modeled in organoids. *Science (New York, N.Y.)* **362**(**6420**):1–9 DOI 10.1126/science.aat6720.

Baquet ZC, Gorski JA, Jones KR. 2004. Early striatal dendrite deficits followed by neuron loss with advanced age in the absence of anterograde cortical brain-derived neurotrophic factor. *The Journal of Neuroscience* **24**(**17**):4250–4258 DOI 10.1523/JNEUROSCI.3920-03.2004.

Bhatt M, Gauthier-Manuel L, Lazzarin E, Zerlotti R, Ziegler C, Bazzone A, Stockner T, Bossi E. 2023. A comparative review on the well-studied GAT1 and the understudied BGT-1 in the brain. *Frontiers in Physiology* **14**:1145973 DOI 10.3389/fphys.2023.1145973.

Bolger AM, Lohse M, Usadel B. 2014. Trimmomatic: a flexible trimmer for illumina sequence data. *Bioinformatics* **30**(**15**):2114–2120 DOI 10.1093/bioinformatics/btu170.

Brown LS, Foster CG, Courtney J-M, King NE, Howells DW, Sutherland BA. 2019. Pericytes and neurovascular function in the healthy and diseased brain. *Frontiers in Cellular Neuroscience* **13**:282 DOI 10.3389/fncel.2019.00282.

Burute M, Gottimukkala K, Galande S. 2012. Chromatin organizer SATB1 is an important determinant of T-cell differentiation. *Immunology & Cell Biology* **90**(**9**):852–859 DOI 10.1038/icb.2012.28.

Can A, Dao DT, Terrillion CE, Piantadosi SC, Bhat S, Gould TD. 2011. The tail suspension test. *Journal of Visualized Experiments* 3769 DOI 10.3791/3769.

Chen Y, Cao P. 2023. Circ-Bnc2 alleviates neuroinflammation in lps-stimulated microglial cells to inhibit neuron cell apoptosis through regulating miR-497a-5p/HECTD1 axis. *Brain and Behavior* **13**(**5**):e2935 DOI 10.1002/brb3.2935.

Chen Z, Chen W, Li Y, Moos M., Xiao D, Wang C. 2022. Single-nucleus chromatin accessibility and RNA sequencing reveal impaired brain development in prenatally e-Cigarette exposed neonatal rats. *IScience* **25(8)**:104686 DOI 10.1016/j.isci.2022.104686.

Costa GA, De Gusmão Taveiros Silva NK, Marianno P, Chivers P, Bailey A, Camarini R. 2023. Environmental enrichment increased bdnf transcripts in the prefrontal cortex: implications for an epigenetically controlled mechanism. *Neuroscience* **526**:277–289 DOI 10.1016/j.neuroscience.2023.07.001.

Cunha C, Brambilla R, Thomas KL. 2010. A simple role for BDNF in learning and memory? *Frontiers in Molecular Neuroscience* **3**:1.

Daimon T. 2011. Box–Cox transformation. In: Lovric M, ed. *International encyclopedia of statistical science.* Berlin, Heidelberg: Springer Berlin Heidelberg, 176–178 DOI 10.1007/978-3-642-04898-2_1.

Dore-Duffy P. 2008. Pericytes: pluripotent cells of the blood brain barrier. *Current Pharmaceutical Design* **14(16)**:1581–1593 DOI 10.2174/138161208784705469.

Fong MF, Mitchell DE, Duffy KR, Bear MF. 2016. Rapid recovery from the effects of early monocular deprivation is enabled by temporary inactivation of the retinas. *Proceedings of the National Academy of Sciences of the United States of America* **113(49)**:14139–14144 DOI 10.1073/pnas.1613279113.

García-Solaesa V, Sanz-Lozano C, Padrón-Morales J, Hernández-Hernández L, García-Sánchez A, Rivera-Reigada M, Dávila-González I, Lorente-Toledano F, Isidoro-García M. 2014. The prostaglandin D2 receptor (PTGDR) gene in asthma and allergic diseases. *Allergologia Et Immunopathologia* **42(1)**:64–68 DOI 10.1016/j.aller.2012.12.002.

Glerup S, Bolcho U, Molgaard S, Boggild S, Vaegter CB, Smith AH, Nieto-Gonzalez JL, Ovesen PL, Pedersen LF, Fjorback AN, Kjolby M, Login H, Holm MM, Andersen OM, Nyengaard JR, Willnow TE, Jensen K, Nykjaer A. 2016. SorCS2 is required for BDNF-dependent plasticity in the hippocampus. *Molecular Psychiatry* **21(12)**:1740–1751 DOI 10.1038/mp.2016.108.

Glerup S, Nykjaer A, Vaegter CB. 2014. Sortilins in neurotrophic factor signaling. *Handbook of Experimental Pharmacology* **220**:165–189 DOI 10.1007/978-3-642-45106-5_7.

Glerup S, Olsen D, Vaegter CB, Gustafsen C, Sjoegaard SS, Hermey G, Kjolby M, Molgaard S, Ulrichsen M, Boggild S, Skeldal S, Fjorback AN, Nyengaard JR, Jacobsen J, Bender D, Bjarkam CR, Sorensen ES, Fuchtbauer EM, Eichele G, Madsen P, Willnow TE, Petersen CM, Nykjaer A. 2014. SorCS2 regulates dopaminergic wiring and is processed into an apoptotic two-chain receptor in peripheral glia. *Neuron* **82(5)**:1074–1087 DOI 10.1016/j.neuron.2014.04.022.

Goodspeed K, Mosca LR, Weitzel NC, Horning K, Simon EW, Pfalzer AC, Xia M, Langer K, Freed A, Bone M, Picone M, Bichell TJV. 2023. A draft conceptual model of SLC6A1 neurodevelopmental disorder. *Frontiers in Neuroscience* **16**:1026065 DOI 10.3389/fnins.2022.1026065.

Hao Y, Hao S, Andersen-Nissen E, Mauck WM, Zheng S, Butler A, Lee MJ, Wilk AJ, Darby C, Zager M, Hoffman P, Stoeckius M, Papalexi E, Mimitou EP, Jain J, Srivastava A, Stuart T, Fleming LM, Yeung B, Rogers AJ, McElrath JM, Blish CA,

Gottardo R, Smibert P, Satija R. 2021. Integrated analysis of multimodal single-cell data. *Cell* **184(13)**:3573–3587.e29 DOI 10.1016/j.cell.2021.04.048.

Hare BD, Duman RS. 2020. Prefrontal cortex circuits in depression and anxiety: contribution of discrete neuronal populations and target regions. *Molecular Psychiatry* DOI 10.1038/s41380-020-0685-9.

Harvey TJ, Davila RA, Vidovic D, Sharmin S, Piper M, Simmons DG. 2021. Genome-wide transcriptomic analysis of the forebrain of postnatal Slc13a4+/- mice. *BMC Research Notes* **14(1)**:269 DOI 10.1186/s13104-021-05687-5.

Johannesen KM, Nielsen J, Sabers A, Isidor B, Kattentidt-Mouravieva AA, Zieglgäns-berger D, Heidlebaugh AR, Oetjens KF, Vidal AA, Christensen J., Tiller J, Freed AN, Møller RS, Rubboli G. 2023. The phenotypic presentation of adult individuals with SLC6A1-related neurodevelopmental disorders. *Frontiers in Neuroscience* **17**:1216653 DOI 10.3389/fnins.2023.1216653.

José C. Pinheiro DB. 2000. Mixed-effects models in S and S-PLUS. *Statistics and computing*, New York: Springer-Verlag.

Kemppainen S, Rantamaki T, Jeronimo-Santos A, Lavasseur G, Autio H, Karpova N, Karkkainen E, Staven S, Vicente Miranda H, Outeiro TF, Diogenes MJ, Laroche S, Davis S, Sebastiao AM, Castren E, Tanila H. 2012. Impaired TrkB receptor signaling contributes to memory impairment in APP/PS1 mice. *Neurobiology of Aging* **33(6)**:1122 e23–39 DOI 10.1016/j.neurobiolaging.2011.11.006.

Khazipov R, Zaynutdinova D, Ogievetsky E, Valeeva G, Mitrukhina O, Manent J-B, Represa A. 2015. Atlas of the postnatal rat brain in stereotaxic coordinates. *Frontiers in Neuroanatomy* **9**:1–5 DOI 10.3389/fnana.2015.00161.

Kida S, Steart PV, Zhang E-T, Weller RO. 1993. Perivascular cells act as scavengers in the cerebral perivascular spaces and remain distinct from pericytes, microglia and macrophages. *Acta Neuropathologica* **85(6)**:646–652 DOI 10.1007/BF00334675.

Kim D, Langmead B, Salzberg SL. 2015. HISAT: a fast spliced aligner with low memory requirements. *Nature Methods* **12(4)**:357–360 DOI 10.1038/nmeth.3317.

Kraemer BR, Snow JP, Vollbrecht P, Pathak A, Valentine WM, Deutch AY, Carter BD. 2014. A role for the P75 neurotrophin receptor in axonal degeneration and apoptosis induced by oxidative stress. *The Journal of Biological Chemistry* **289(31)**:21205–21216 DOI 10.1074/jbc.M114.563403.

Lanshakov DA, Sukhareva EV, Bulygina VV, Bannova AV, Shaburova EV, Kalinina TS. 2021. Single neonatal dexamethasone administration has long-lasting outcome on depressive-like behaviour, Bdnf, Nt-3, P75ngfr and sorting receptors (SorCS1-3) stress reactive expression. *Scientific Reports* **11(1)**:8092 DOI 10.1038/s41598-021-87652-7.

Lanshakov DA, Sukhareva EV, Kalinina TS, Dygalo NN. 2016. Dexamethasone-induced acute excitotoxic cell death in the developing brain. *Neurobiology of Disease* **91**:1–9 DOI 10.1016/j.nbd.2016.02.009.

Leloup N, Chataigner LMP, Janssen BJC. 2018. Structural insights into SorCS2-nerve growth factor complex formation. *Nature Communications* **9(1)**:2979 DOI 10.1038/s41467-018-05405-z.

Liao Y, Smyth GK, Shi W. 2019. The R package rsubread is easier, faster, cheaper and better for alignment and quantification of RNA sequencing reads. *Nucleic Acids Research* **47(8)**:e47 DOI 10.1093/nar/gkz114.

Lojewski X, Srimasorn S, Rauh J, Francke S, Wobus M, Taylor V, Araúzo-Bravo MJ, Hallmeyer-Elgner S, Kirsch M, Schwarz S, Schwarz J, Storch A, Hermann A. 2015. Perivascular mesenchymal stem cells from the adult human brain harbor no instrinsic neuroectodermal but high mesodermal differentiation potential. *Stem Cells Translational Medicine* **4(10)**:1223–1233 DOI 10.5966/sctm.2015-0057.

Luhmann HJ, Sinning A, Yang JW, Reyes-Puerta V, Stuttgen MC, Kirischuk S, Kilb W. 2016. Spontaneous neuronal activity in developing neocortical networks: from single cells to large-scale interactions. *Frontiers in Neural Circuits* **10**:40 DOI 10.3389/fncir.2016.00040.

Marchetti L, Bonsignore F, Gobbo F, Amodeo R, Calvello M, Jacob A, Signore G, Schirripa Spagnolo C, Porciani D, Mainardi M, Beltram F, Luin S, Cattaneo A. 2019. Fast-diffusing P75(NTR) monomers support apoptosis and growth cone collapse by neurotrophin ligands. *Proceedings of the National Academy of Sciences of the United States of America* **116(43)**:21563–21572 DOI 10.1073/pnas.1902790116.

Marín-Méndez JJ, Patiño-García A, Segura V, Ortuño F, Gálvez MD, Soutullo CA. 2012. Differential expression of prostaglandin D2 synthase (PTGDS) in patients with attention deficit–hyperactivity disorder and bipolar disorder. *Journal of Affective Disorders* **138(3)**:479–484 DOI 10.1016/j.jad.2012.01.040.

McCarthy DJ, Chen Y, Smyth GK. 2012. Differential expression analysis of multifactor RNA-Seq experiments with respect to biological variation. *Nucleic Acids Research* **40(10)**:4288–4297 DOI 10.1093/nar/gks042.

Melby L, Indredavik MS, Lohaugen G, Brubakk AM, Skranes J, Vik T. 2020. Is there an association between full IQ score and mental health problems in young adults? A study with a convenience sample. *BMC Psychology* **8(1)**:7 DOI 10.1186/s40359-020-0372-2.

Menshanov PN, Lanshakov DA, Dygalo NN. 2015. proBDNF is a major product of Bdnf gene expressed in the perinatal rat cortex. *Physiological Research* 925–934 DOI 10.33549/physiolres.932996.

Minichiello L. 2009. TrkB signalling pathways in LTP and learning. *Nature Reviews. Neuroscience* **10(12)**:850–860 DOI 10.1038/nrn2738.

Miranda M, Morici JF, Zanoni MB, Bekinschtein P. 2019. Brain-derived neurotrophic factor: a key molecule for memory in the healthy and the pathological brain. *Frontiers in Cellular Neuroscience* **13**:363 DOI 10.3389/fncel.2019.00363.

Mohri I, Kadoyama K, Kanekiyo T, Sato Y, Kagitani-Shimono K, Saito Y, Suzuki K, Kudo T, Takeda M, Urade Y, Murayama S, Taniike M. 2007. Hematopoietic prostaglandin D synthase and DP1 receptor are selectively upregulated in microglia and astrocytes within senile plaques from human patients and in a mouse model of Alzheimer disease. *Journal of Neuropathology and Experimental Neurology* **66(6)**:469–480 DOI 10.1097/01.jnen.0000240472.43038.27.

Mowla SJ, Farhadi HF, Pareek S, Atwal JK, Morris SJ, Seidah NG, Murphy RA. 2001. Biosynthesis and post-translational processing of the precursor to brain-derived neurotrophic factor. *The Journal of Biological Chemistry* **276**(**16**):12660–12666 DOI 10.1074/jbc.M008104200.

Munkholm K, Peijs L, Kessing LV, Vinberg M. 2015. Reduced mRNA expression of PTGDS in peripheral blood mononuclear cells of rapid-cycling bipolar disorder patients compared with healthy control subjects. *International Journal of Neuropsychopharmacology* **18**(**5**):pyu101–pyu101 DOI 10.1093/ijnp/pyu101.

Nadjar Y, Triller A, Bessereau J-L, Dumoulin A. 2015. The Susd2 protein regulates neurite growth and excitatory synaptic density in hippocampal cultures. *Molecular and Cellular Neuroscience* **65**:82–91 DOI 10.1016/j.mcn.2015.02.007.

Narayanan SN, Kumar RS. 2018. An improved light dark box test by using a real-time video tracking system. *Acta Biologica Hungarica* **69**(**4**):371–384 DOI 10.1556/018.69.2018.4.1.

Pahl A. 2007. Prostaglandin-D synthase. In: *xPharm: the comprehensive pharmacology reference.* Cambridge, MA: United States Elsevier Inc. (S&T Books and Cell Press), 1–5 DOI 10.1016/B978-008055232-3.63685-2.

Parker JL, Kato T, Kuteyi G, Sitsel O, Newstead S. 2023. Molecular basis for selective uptake and elimination of organic anions in the kidney by OAT1. *Nature Structural & Molecular Biology* **30**(**11**):1786–1793 DOI 10.1038/s41594-023-01039-y.

Paul G, Özen I, Christophersen NS, Reinbothe T, Bengzon J, Visse E, Jansson K, Dannaeus K, Henriques-Oliveira C, Roybon L, Anisimov SV, Renström E, Svensson M, Haegerstrand A, Brundin P. 2012. The adult human brain harbors multipotent perivascular mesenchymal stem cells. *PLOS ONE* **7**(**4**):e35577 DOI 10.1371/journal.pone.0035577.

Phillips C. 2017. Brain-derived neurotrophic factor, depression, and physical activity: making the neuroplastic connection. *Neural Plasticity* **2017**:7260130 DOI 10.1155/2017/7260130.

Pizzorusso T, Medini P, Landi S, Baldini S, Berardi N, Maffei L. 2006. Structural and functional recovery from early monocular deprivation in adult rats. *Proceedings of the National Academy of Sciences of the United States of America* **103**(**22**):8517–8522 DOI 10.1073/pnas.0602657103.

Polioudakis D, De la Torre-Ubieta L, Langerman J, Elkins AG, Shi X, Stein JL, Vuong CK, Nichterwitz S, Gevorgian M, Opland CK, Lu D, Connell W, Ruzzo EK, Lowe JK, Hadzic T, Hinz FI, Sabri S, Lowry WE, Gerstein MB, Plath K, Geschwind DH. 2019. A single-cell transcriptomic atlas of human neocortical development during mid-gestation. *Neuron* **103**(**5**):785–801 e8 DOI 10.1016/j.neuron.2019.06.011.

Pujol-Gualdo N, Sánchez-Mora C, Ramos-Quiroga JA, Ribasés M, Soler Artigas M. 2021. Integrating genomics and transcriptomics: towards deciphering ADHD. *European Neuropsychopharmacology* **44**:1–13 DOI 10.1016/j.euroneuro.2021.01.002.

QuPath. 2024. Multiplexed analysis. *Available at https://qupath.readthedocs.io/en/stable/docs/tutorials/multiplex_analysis.html.*

Rajakariar R, Hilliard M, Lawrence T, Trivedi S, Colville-Nash P, Bellingan G, Fitzgerald D, Yaqoob MM, Gilroy DW. 2007. Hematopoietic prostaglandin D_2 synthase controls the onset and resolution of acute inflammation through PGD_2 and 15-deoxy Δ^{12-14} PGJ_2. *Proceedings of the National Academy of Sciences of the United States of America* **104(52)**:20979–20984 DOI 10.1073/pnas.0707394104.

Rakoczy J, Zhang Z, Bowling FG, Dawson PA, Simmons DG. 2015. Loss of the sulfate transporter Slc13a4 in placenta causes severe fetal abnormalities and death in mice. *Cell Research* **25(11)**:1273–1276 DOI 10.1038/cr.2015.100.

Rezgaoui M, Hermey G, Riedel IB, Hampe W, Schaller HC, Hermans-Borgmeyer I. 2001. Identification of SorCS2, a novel member of the VPS10 domain containing receptor family, prominently expressed in the developing mouse brain. *Mechanisms of Development* **100(2)**:335–338 DOI 10.1016/S0925-4773(00)00523-2.

Rustenhoven J, Jansson D, Smyth LC, Dragunow M. 2017. Brain pericytes as mediators of neuroinflammation. *Trends in Pharmacological Sciences* **38(3)**:291–304 DOI 10.1016/j.tips.2016.12.001.

Satinsky EN, Kakuhikire B, Baguma C, Rasmussen JD, Ashaba S, Cooper-Vince CE, Perkins JM, Kiconco A, Namara EB, Bangsberg DR, Tsai AC. 2021. Adverse childhood experiences, adult depression, and suicidal ideation in rural uganda: a cross-sectional, population-based study. *PLOS Medicine* **18(5)**:e1003642 DOI 10.1371/journal.pmed.1003642.

Searle SR, Speed FM, Milliken GA. 1980. Population marginal means in the linear model: an alternative to least squares means. *The American Statistician* **34(4)**:216–221 DOI 10.1080/00031305.1980.10483031.

Shaburova EV, Lanshakov DA. 2021. Effective transduction of brain neurons with lentiviral vectors purified via ion-exchange chromatography. *Applied Biochemistry and Microbiology* **57(8)**:890–898 DOI 10.1134/S0003683821080044.

Shibata M, Pattabiraman K, Lorente-Galdos B, Andrijevic D, Kim S-K, Kaur N, Muchnik SK, Xing X, Santpere G, Sousa AMM, Sestan N. 2021. Regulation of prefrontal patterning and connectivity by retinoic acid. *Nature* **598(7881)**:483–488 DOI 10.1038/s41586-021-03953-x.

Shibata M, Pattabiraman K, Lorente-Galdos B, Andrijevic D, Xing X, Sousa AMM, Santpere G, Sestan N. 2019. Regulation of prefrontal patterning, connectivity and synaptogenesis by retinoic acid DOI 10.1101/2019.12.31.891036.

Wahab A, Almangush A, Andersson LC, Nieminen P, Salo T. 2020. Impact of astroprincin (FAM171A1) expression in oral tongue cancer. *Frontiers in Oral Health* **1**:599421 DOI 10.3389/froh.2020.599421.

Watson AJ, Henson K, Dorsey SG, Frank MG. 2015. The truncated TrkB receptor influences mammalian sleep. *American Journal of Physiology. Regulatory, Integrative and Comparative Physiology* **308(3)**:R199–R207 DOI 10.1152/ajpregu.00422.2014.

Weaver ICG, Cervoni N, Champagne FA, D'Alessio AC, Sharma S, Seckl JR, Dymov S, Szyf M, Meaney MJ. 2004. Epigenetic programming by maternal behavior. *Nature Neuroscience* **7(8)**:847–854 DOI 10.1038/nn1276.

Weinsheimer S, Bendjilali N, Nelson J, Guo DE, Zaroff JG, Sidney S, McCulloch CE, Al-Shahi Salman R, Berg JN, Koeleman BPC, Simon M, Bostroem A, Fontanella M, Sturiale CL, Pola R, Puca A, Lawton MT, Young WL, Pawlikowska L, Klijn CJM, Kim H. 2016. Genome-wide association study of sporadic brain arteriovenous malformations. *Journal of Neurology, Neurosurgery & Psychiatry* **87**(**9**):916–923 DOI 10.1136/jnnp-2015-312272.

Wu T, Hu E, Xu S, Chen M, Guo P, Dai Z, Feng T, Zhou L, Tang W, Zhan L, Fu X, Liu S, Bo X, Yu G. 2021. clusterProfiler 4.0: a universal enrichment tool for interpreting omics data. *The Innovation* **2**(**3**):100141 DOI 10.1016/j.xinn.2021.100141.

Xia Y, Wang G, Xiao L, Du Y, Lin S, Nan C, Weng S. 2023. Effects of early adverse life events on depression and cognitive performance from the perspective of the heart-brain axis. *Brain Sciences* **13**(**8**):1174 DOI 10.3390/brainsci13081174.

Yang J, Zaitlen NA, Goddard ME, Visscher PM, Price AL. 2014. Advantages and pitfalls in the application of mixed-model association methods. *Nature Genetics* **46**(**2**):100–106 DOI 10.1038/ng.2876.

Zhong S, Zhang S, Fan X, Wu Q, Yan L, Dong J, Zhang H, Li L, Sun L, Pan N, Xu X, Tang F, Zhang J, Qiao J, Wang X. 2018. A single-cell RNA-seq survey of the developmental landscape of the human prefrontal cortex. *Nature* **555**(**7697**):524–528 DOI 10.1038/nature25980.